

000 001 002 003 004 005 006 007 008 009 010 011 012 013 014 015 016 017 018 019 020 021 022 023 024 025 026 027 028 029 030 031 032 033 034 035 036 037 038 039 040 041 042 043 044 045 046 047 048 049 050 051 052 053 MOCHA: MULTI-SAMPLE OMICS COHORTS WITH HUMAN ANNOTATION

Anonymous authors

Paper under double-blind review

ABSTRACT

In spatially resolved transcriptomics (SRT) research, gene expression profiling with spatial context has enabled spatial domain identification within single tissue samples. Extending these analyses to multiple biological samples presents additional challenges, including cross-sample variability and batch effects. Method development has been limited by the lack of datasets that combine multi-subject cohorts with expert-derived annotations. We present MOCHA (Multi-sample Omics Cohorts with Human Annotation), a curated resource for developing and evaluating multi-sample SRT methods. MOCHA integrates molecular profiles, spatial profiles, and high-resolution Hematoxylin and Eosin (H&E) images across multiple subjects, with each sample paired with domain annotations from expert pathologists. For algorithm development and evaluation, MOCHA provides standardized data organization, efficient storage formats for large-scale processing, and protocols for handling batch effects in multi-sample integration.

1 INTRODUCTION

Spatially resolved transcriptomics (SRT) links gene expression profiles to precise tissue coordinates, enabling quantitative analysis of microanatomy and cellular organization at high resolution. Multiple platforms now make SRT broadly accessible, including sequencing-based assays such as 10x Genomics Visium and Slide-seq (Stähli et al., 2016; Tian et al., 2023) and imaging-based assays such as MERFISH (Chen et al., 2015) and STARmap (Wang et al., 2018). The resolution of these technologies varies from multi-cellular spots to near single-cell measurements, but all require computational approaches that can identify coherent tissue domains by combining molecular profiles with spatial information.

Several repositories have been developed to organize publicly available datasets, including SORC for cancer research (Zhou et al., 2024), Aquila for cross-disease analyses (Zheng et al., 2023), and others such as SODB (Yuan et al., 2023), STOmicsDB (Xu et al., 2022), and SpatialDB (Fan et al., 2020). Despite this progress, multi-subject datasets with expert-generated spatial annotations remain limited. This gap constrains systematic method development for multi-sample integration—an essential setting for cohort-level studies that must model biological heterogeneity alongside technical variation.

Methodological advances underscore this need. Early work emphasized single-sample domain identification, including Bayesian modeling approaches such as BayesSpace (Zhao et al., 2021) and deep learning methods that integrate histology, including iIMPACT (Jiang et al., 2024). More recent approaches—such as BASS (Li & Zhou, 2022), BayeSmart (Guo et al., 2024), and graph-based methods like STAGATE (Dong & Zhang, 2022)—extend analysis to multiple samples using distinct strategies, from clustering across tissues to learning shared representations. Additional challenges, such as deconvolution of mixed spots (Chen et al., 2022; 2023; Luo et al., 2024) and correction for batch effects, reinforce the importance of datasets that provide aligned molecular, spatial, and histological information together with expert annotations.

We introduce MOCHA, a Multi-sample Omics Cohorts with Human Annotation database for training and evaluation of multi-sample SRT methods. MOCHA aggregates multi-subject datasets that each include a gene expression matrix, spatial coordinates, and a co-registered high-resolution Hematoxylin and Eosin (H&E) image (Chan, 2014). Each sample is accompanied by spatial domain

054 labels produced by an expert pathologist, enabling evaluation of domain delineation and representation learning in multi-sample contexts. To promote reproducibility and accessibility, MOCHA is
 055 released in formats readily usable with Python and R and distributed for integration into existing
 056 pipelines.
 057

059 2 DATASETS

061 To assemble a resource for multi-sample spatial domain identification, we curated a set of publicly
 062 available SRT datasets. Following an approach similar to that in the STimage-1K4M review Chen
 063 et al. (2024), we systematically searched repositories including 10x Genomics, Gene Expression
 064 Omnibus (GEO), and Spatial Research. Our selection criteria required each study to provide a cell-
 065 by-gene expression count matrix, a spatial coordinate matrix, and cellular annotations delineated by
 066 a pathologist using the corresponding H&E images.
 067

068 This search yielded 10 distinct cohorts, summarized in Table 1. Cancer-related datasets in-
 069 clude HER2-positive breast cancer (BC_HER2+) (Andersson et al., 2021), high-plasticity subtypes
 070 (BC_HP) (Coutant & et al., 2023), recurrent neoplastic heterogeneity (BC_NP) (Wu et al., 2021),
 071 triple-negative breast cancer (BC_TNBC) (Wang et al., 2024), colorectal cancer consensus molecu-
 072 lar subtypes (CRC_CMS) (Valdeolivas et al., 2024), kidney cancer with tertiary lymphoid structures
 073 (KC_TLS) (Dawo et al., 2023), lung cancer with tertiary lymphoid structures (LC_TLS) (Dawo
 074 et al., 2023), and renal cell carcinoma with tertiary lymphoid structures (RCC_TLS) (Meylan &
 075 et al., 2022), along with human dorsolateral prefrontal cortex (DLPFC) (Maynard et al., 2021) and
 076 mouse olfactory bulb (MOB) (Ståhl & et al., 2016).
 077

078 Table 1: A summary of the SRT datasets. (BC: Breast cancer; CRC: Colorectal cancer; DLPFC:
 079 Dorsolateral prefrontal cortex; KC: Kidney cancer; LC: Lung cancer; MOB: Mouse olfactory bulb;
 080 RCC: Renal cell carcinoma)

| Cohort | Tissue | Technology | Subjects | Samples |
|--------------|---|------------|----------|---------|
| BC_HER2+_10x | HER2-positive (HER2+) breast cancer | 10x Visium | 8 | 8 |
| BC_HP_10x | High-plasticity (HP) breast cancer subtypes | 10x Visium | 12 | 14 |
| BC_NP_10x | Recurrent neoplastic (NP) cell heterogeneity in breast cancer | 10x Visium | 6 | 6 |
| BC_TNBC_ST | Triple-negative breast can- cer (TNBC) | ST | 94 | 94 |
| CRC_CMS_10x | Colorectal cancer consen- sus molecular subtypes (CMS) | 10x Visium | 11 | 14 |
| DLPFC_10x | Dorsolateral prefrontal cor- tex | 10x Visium | 3 | 12 |
| KC_TLS_10x | Kidney cancer with tertiary lymphoid structures (TLS) | 10x Visium | 3 | 3 |
| LC_TLS_10x | Lung cancer with tertiary lymphoid structures (TLS) | 10x Visium | 5 | 5 |
| MOB_ST | Mouse olfactory bulb | ST | 1 | 12 |
| RCC_TLS_10x | Tertiary lymphoid struc- tures (TLS) in renal cell carcinoma | 10x Visium | 23 | 23 |

101
 102 These cohorts span a wide range of tissue types and disease contexts, encompassing both human and
 103 mouse studies, and multiple technological platforms (10x Genomics Visium and ST). The scale also
 104 varies substantially, with BC_TNBC including 94 subjects and 94 samples, while smaller datasets
 105 such as KC_TLS and LC_TLS consist of only three and five samples, respectively. Together, these
 106 datasets enable evaluation of multi-sample spatial domain identification methods. A summary of
 107 molecular characteristics, including the number of spots, genes, and data sparsity for each cohort, is
 108 presented in Figure 1.

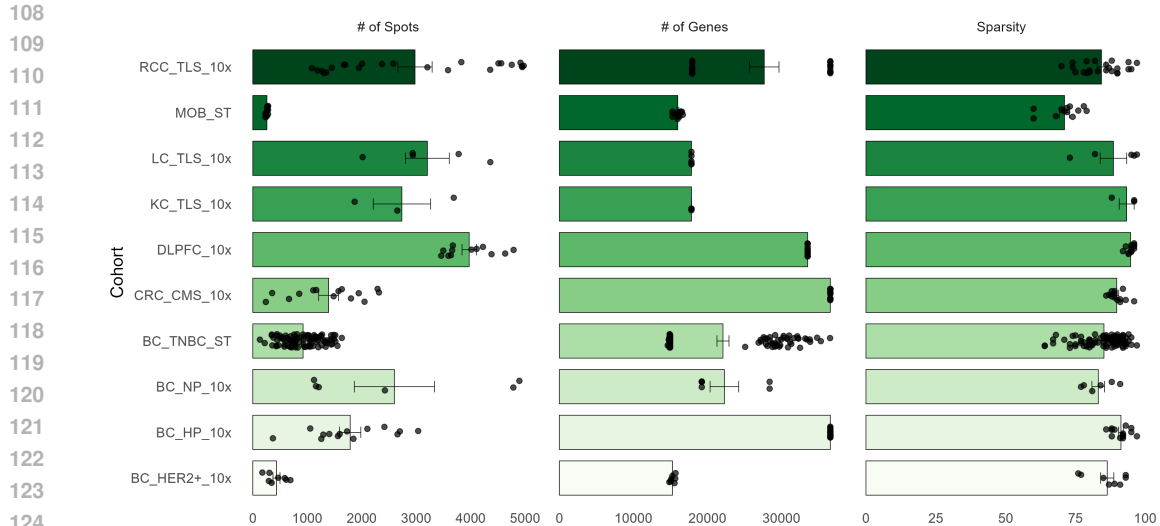


Figure 1: A summary of the molecular profiles for each cohort.

3 PRE-PROCESSING AND BATCH EFFECT CORRECTION

A standard pipeline for preprocessing multi-sample SRT data starts by concatenating the raw gene expression matrices from each sample over a set of common genes, followed by library size normalization to correct for variability in sequencing depth. This adjustment can be performed using packages such as `scater` and `scran`, which implement techniques such as the trimmed mean of M-values (TMM), relative log expression (RLE), and upper-quartile scaling (Robinson & Oshlack, 2010; Anders & Huber, 2010; Bullard et al., 2010; McCarthy et al., 2017). Alternatively, frameworks such as `Seurat` and `scanpy` apply a global-scaling approach in which counts for each cell are divided by the total count, rescaled to a fixed scaling factor (e.g., 10,000), and log-transformed to stabilize variance (Hao et al., 2023; Wolf et al., 2018).

Following normalization, dimensionality reduction can be performed through feature selection or projection methods. Feature selection can involve identifying spatially variable genes (SVGs) using methods such as SPARK-X (Zhu et al., 2021; Zhao et al., 2021; Jiang et al., 2024), or highly variable genes (HVGs), which are generally preferred in studies involving multiple subjects to reduce inter-subject variability (Li & Zhou, 2022). Dimensionality reduction can also be achieved by projecting the data into a lower-dimensional space using techniques such as PCA, t-SNE, UMAP, or graph attention autoencoders as implemented in STAGATE (van der Maaten & Hinton, 2008; Becht et al., 2019; Dong & Zhang, 2022).

Batch correction can be subsequently performed to adjust for systematic variation between samples. One common approach is to operate on reduced feature spaces using techniques such as Harmony (Korsunsky et al., 2019; Li & Zhou, 2022; Guo et al., 2024). An overview of this batch effect correction, and feature selection, workflow is demonstrated in Figure 2.

An alternative pipeline for batch correction is implemented in Crescendo, which avoids transformation to a reduced-dimensional space and instead models the raw, integer-valued counts directly (Millard et al., 2025). This approach employs a generalized linear mixed model (GLMM) in which the batch is included as a random effect, preserving the discrete structure of the data. Crescendo can extend single-sample spatial clustering models such as BayesCafe, which relies on the zero-inflated negative binomial (ZINB) distribution (Li et al., 2024), to multi-sample settings by integrating batch correction directly within the generative hierarchy.

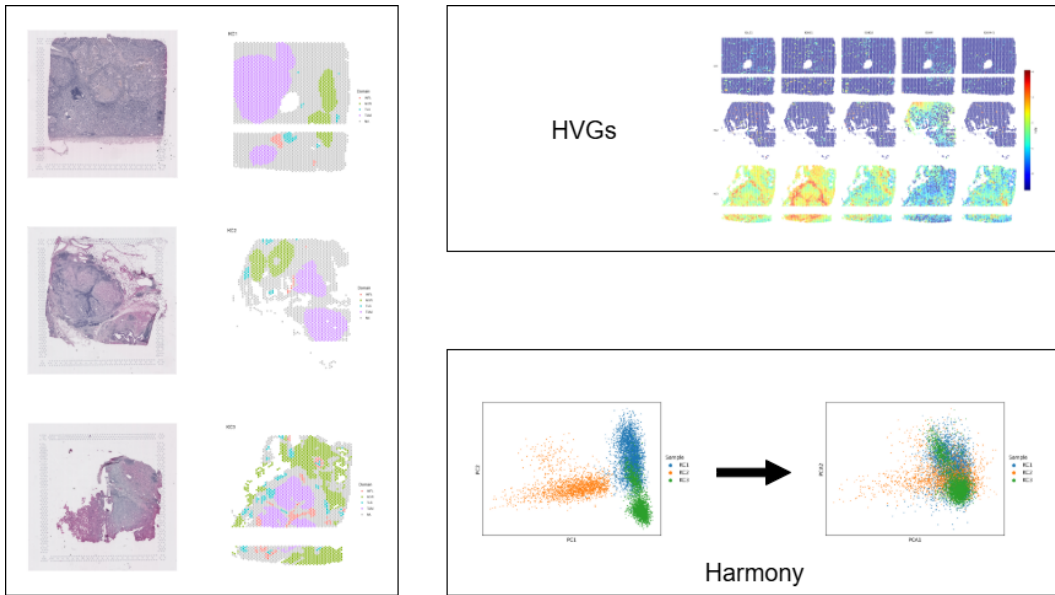


Figure 2: AA standard pipeline for feature selection with HVGs and batch effect correction using Harmony, illustrated with the KC_TLS_10x cohort (Dawo et al., 2023).

4 MULTI-SAMPLE SPATIAL CLUSTERING METHODS

Recent advances in computational modeling have led to methods that extend spatial transcriptomics analysis from single-sample to multi-sample settings. These approaches are designed to integrate spatial and molecular information across subjects while accounting for technical and biological variability.

As summarized in Table 2, BayeSMART is a Bayesian framework for multi-sample spatial clustering that integrates reconstructed single-cell information from histology images with spatial gene expression (Guo et al., 2024). BASS is a hierarchical Bayesian model that jointly performs cell type clustering and spatial domain identification across samples (Li & Zhou, 2022). STAGATE is a graph attention autoencoder that generates low-dimensional embeddings by combining spatial neighborhood structure with molecular profiles (Dong & Zhang, 2022).

Table 2: A summary of the existing multi-sample spatial clustering methods. These Bayesian (Bayes) or deep learning (DL) approaches use Principal Component Analysis (PCA) or autoencoders (AE) for dimension reduction. Additionally, BayeSMART integrates information from H&E images.

| Method | Dimension reduction | H&E | Approach | Language | Year |
|-----------|---------------------|-----|----------|----------|------|
| BayeSMART | PCA | ✓ | Bayes | R/C++ | 2024 |
| BASS | PCA | | Bayes | R/C++ | 2022 |
| STAGATE | AE | | DL | Python | 2022 |

In a majority of the cancer studies included in MOCHA, the detailed pathologist annotations can be grouped into four broad categories: immune, stroma, tumor, and normal. These groupings, described in the Supplementary Material, provide a consistent reference structure for applying multi-sample spatial clustering methods while accommodating variability across cohorts.

216 AUTHOR CONTRIBUTIONS

217

218 ACKNOWLEDGMENTS

219

220 REFERENCES

221 Simon Anders and Wolfgang Huber. Differential expression analysis for sequence count data.
 222 *Genome Biology*, 11(10):R106, 2010. doi: 10.1186/gb-2010-11-10-r106. URL <https://doi.org/10.1186/gb-2010-11-10-r106>.

224 A. Andersson, L. Larsson, L. Stenbeck, and et al. Spatial deconvolution of her2-positive breast cancer delineates tumor-associated cell type interactions. *Nature Communications*, 12:6012, 2021.
 225 doi: 10.1038/s41467-021-26271-2.

228 Etienne Becht, Leland McInnes, John Healy, and et al. Dimensionality reduction for visualizing
 229 single-cell data using umap. *Nature Biotechnology*, 37:38–44, 2019. doi: 10.1038/nbt.4314.
 230 URL <https://doi.org/10.1038/nbt.4314>.

231 James H. Bullard, Elizabeth Purdom, Kasper D. Hansen, and Sandrine Dudoit. Evaluation of
 232 statistical methods for normalization and differential expression in mrna-seq experiments. *BMC
 233 Bioinformatics*, 11(94):1–13, 2010. doi: 10.1186/1471-2105-11-94. URL <https://doi.org/10.1186/1471-2105-11-94>.

235 J. K. C. Chan. The wonderful colors of the hematoxylin–eosin stain in diagnostic surgical
 236 pathology. *International Journal of Surgical Pathology*, 22(1):12–32, 2014. doi: 10.1177/
 237 1066896913517939. URL <https://doi.org/10.1177/1066896913517939>.

238 J. Chen, W. Liu, T. Luo, Z. Yu, M. Jiang, J. Wen, G. P. Gupta, P. Giusti, H. Zhu, Y. Yang, et al.
 239 A comprehensive comparison on cell-type composition inference for spatial transcriptomics data.
 240 *Briefings in Bioinformatics*, 23(4):bbac245, 2022. doi: 10.1093/bib/bbac245. URL <https://doi.org/10.1093/bib/bbac245>.

243 J. Chen, T. Luo, M. Jiang, J. Liu, G. P. Gupta, and Y. Li. Cell composition inference and iden-
 244 tification of layer-specific spatial transcriptional profiles with polaris. *Science Advances*, 9
 245 (9):eadd9818, 2023. doi: 10.1126/sciadv.add9818. URL <https://doi.org/10.1126/sciadv.add9818>.

247 J. Chen, M. Zhou, W. Wu, J. Zhang, Y. Li, and D. Li. Stimage-1k4m: A histopathology image-
 248 gene expression dataset for spatial transcriptomics. *arXiv preprint*, jun 2024. URL <https://arxiv.org/abs/2406.06393>. PMID: 38947920; PMCID: PMC11213178.

250 K. H. Chen, A. N. Boettiger, J. R. Moffitt, S. Wang, and X. Zhuang. Spatially resolved, highly
 251 multiplexed rna profiling in single cells. *Science*, 348(6233):aaa6090, apr 2015. doi: 10.1126/
 252 science.aaa6090. URL <https://doi.org/10.1126/science.aaa6090>.

254 Angèle Coutant and et al. Spatial transcriptomics reveal pitfalls and opportunities for the detection
 255 of rare high-plasticity breast cancer subtypes. *Laboratory Investigation*, 103(12):100258, 2023.

256 Sebastian Dawo, Kalin Nonchev, and Karina Silina. 10x visium spatial transcriptomics dataset:
 257 Kidney (3) and lung (5) cancer with tertiary lymphoid structures. <https://zenodo.org/records/14620362>, 2023.

259 Ke Dong and Shihua Zhang. Deciphering spatial domains from spatially resolved transcrip-
 260 toomics with an adaptive graph attention auto-encoder. *Nature Communications*, 13(1):1739,
 261 Apr 2022. doi: 10.1038/s41467-022-29439-6. URL <https://doi.org/10.1038/s41467-022-29439-6>.

263 Zhen Fan, Runsheng Chen, and Xiaowei Chen. Spatialldb: a database for spatially resolved trans-
 264 scriptomes. *Nucleic Acids Research*, 48(D1):D233–D237, jan 2020. doi: 10.1093/nar/gkz934.
 265 URL <https://doi.org/10.1093/nar/gkz934>.

267 Yanghong Guo, Bencong Zhu, Chen Tang, Ruichen Rong, Ying Ma, Guanghua Xiao, Lin Xu, and
 268 Qiwei Li. BayeSMART: Bayesian clustering of multi-sample spatially resolved transcriptomics
 269 data. *Briefings in Bioinformatics*, 25(6):bbae524, Nov 2024. doi: 10.1093/bib/bbae524. URL
<https://doi.org/10.1093/bib/bbae524>.

270 Yuhao Hao, Tim Stuart, Michael H Kowalski, Sagar Choudhary, Paul Hoffman, et al. Dictionary
 271 learning for integrative, multimodal and scalable single-cell analysis. *Nature Biotechnology*, 2023. doi: 10.1038/s41587-023-01767-y. URL <https://doi.org/10.1038/s41587-023-01767-y>.

272

273

274 Xin Jiang, Shuang Wang, Li Guo, and et al. iimpact: integrating image and molecular profiles
 275 for spatial transcriptomics analysis. *Genome Biology*, 25:147, 2024. doi: 10.1186/s13059-024-03289-5. URL <https://doi.org/10.1186/s13059-024-03289-5>.

276

277

278 Ilya Korsunsky, Neil Millard, Jian Fan, and et al. Fast, sensitive and accurate integration of single-
 279 cell data with harmony. *Nature Methods*, 16:1289–1296, 2019. doi: 10.1038/s41592-019-0619-0.
 280 URL <https://doi.org/10.1038/s41592-019-0619-0>.

281

282 Huimin Li, Bencong Zhu, Xi Jiang, Lei Guo, Yang Xie, Lin Xu, and Qiwei Li. An interpretable
 283 bayesian clustering approach with feature selection for analyzing spatially resolved transcriptomics
 284 data. *Biometrics*, 80(3):ujae066, September 2024. doi: 10.1093/biometc/ujae066. URL
 285 <https://doi.org/10.1093/biometc/ujae066>.

286

287 Zhi Li and Xiang Zhou. Bass: multi-scale and multi-sample analysis enables accurate cell type
 288 clustering and spatial domain detection in spatial transcriptomic studies. *Genome Biology*,
 289 23:168, 2022. doi: 10.1186/s13059-022-02734-7. URL <https://doi.org/10.1186/s13059-022-02734-7>.

290

291 T. Luo, J. Chen, W. Wu, J. Zhao, H. Yao, H. Zhu, and Y. Li. Mast-decon: Smooth cell-type decon-
 292 volution method for spatial transcriptomics data. *bioRxiv*, pp. 2024–05, 2024. doi: 10.1101/2024.
 293 05.03.592867. URL <https://doi.org/10.1101/2024.05.03.592867>.

294

295 K.R. Maynard, L. Collado-Torres, L.M. Weber, and et al. Transcriptome-scale spatial gene expres-
 296 sion in the human dorsolateral prefrontal cortex. *Nature Neuroscience*, 24:425–436, 2021. doi:
 297 10.1038/s41593-020-00787-0.

298

299 Davis J. McCarthy, Kieran R. Campbell, Aaron T. L. Lun, and Quin F. Wills. Scater: pre-processing,
 300 quality control, normalization and visualization of single-cell rna-seq data in r. *Bioinformatics*, 33
 301 (8):1179–1186, April 2017. doi: 10.1093/bioinformatics/btw777. URL <https://doi.org/10.1093/bioinformatics/btw777>.

302

303 Maxime Meylan and et al. Tertiary lymphoid structures generate and propagate anti-tumor antibody-
 304 producing plasma cells in renal cell cancer. *Immunity*, 55(3):527–541.e5, 2022.

305

306 Neil Millard, Jhen Hwa Chen, Mukta G. Palshikar, and et al. Batch correcting single-cell spatial
 307 transcriptomics count data with crescendo improves visualization and detection of spatial gene
 308 patterns. *Genome Biology*, 26:36, 2025. doi: 10.1186/s13059-025-03479-9. URL <https://doi.org/10.1186/s13059-025-03479-9>.

309

310 Mark D. Robinson and Alicia Oshlack. A scaling normalization method for differential expression
 311 analysis of rna-seq data. *Genome Biology*, 11(3):R25, 2010. doi: 10.1186/gb-2010-11-3-r25.
 312 URL <https://doi.org/10.1186/gb-2010-11-3-r25>.

313

314 P. L. Ståhl, F. Salmén, S. Vickovic, A. Lundmark, J. F. Navarro, J. Magnusson, S. Giacomello,
 315 M. Asp, J. O. Westholm, M. Huss, et al. Visualization and analysis of gene expression in tissue
 316 sections by spatial transcriptomics. *Science*, 353(6294):78–82, jul 2016. doi: 10.1126/science.
 317 aaf2403. URL <https://doi.org/10.1126/science.aaf2403>.

318

319 Patrik L. Ståhl and et al. Visualization and analysis of gene expression in tissue sections by spatial
 320 transcriptomics. *Science*, 353:78–82, 2016. doi: 10.1126/science.aaf2403.

321

322 L. Tian, F. Chen, and E. Z. Macosko. The expanding vistas of spatial transcriptomics. *Nature
 323 Biotechnology*, 41(6):773–782, jun 2023. doi: 10.1038/s41587-023-01792-0. URL <https://doi.org/10.1038/s41587-023-01792-0>.

324

325 A. Valdeolivas, B. Amberg, N. Giroud, and et al. Profiling the heterogeneity of colorectal cancer
 326 consensus molecular subtypes using spatial transcriptomics. *npj Precision Oncology*, 8:10, 2024.
 327 doi: 10.1038/s41698-023-00488-4.

324 Laurens van der Maaten and Geoffrey Hinton. Visualizing data using t-sne. *Journal of Ma-
325 chine Learning Research*, 9:2579–2605, 2008. URL <http://www.jmlr.org/papers/v9/vandermaaten08a.html>.

326

327 X. Wang, W. E. Allen, M. A. Wright, E. L. Sylwestrak, N. Samusik, S. Vesuna, K. Evans, C. Liu,
328 C. Ramakrishnan, J. Liu, et al. Three-dimensional intact-tissue sequencing of single-cell tran-
329 scriptional states. *Science*, 361(6400):eaat5691, jul 2018. doi: 10.1126/science.aat5691. URL
330 <https://doi.org/10.1126/science.aat5691>.

331

332 X. Wang, D. Venet, F. Liffrange, and et al. Spatial transcriptomics reveals substantial heterogeneity
333 in triple-negative breast cancer with potential clinical implications. *Nature Communications*, 15:
334 10232, 2024. doi: 10.1038/s41467-024-54145-w.

335

336 Fabian A Wolf, Philipp Angerer, and Fabian J Theis. SCANPY: large-scale single-cell gene expres-
337 sion data analysis. *Genome Biology*, 19(1):15, 2018. doi: 10.1186/s13059-017-1382-0. URL
338 <https://doi.org/10.1186/s13059-017-1382-0>.

339

340 S.Z. Wu, G. Al-Eryani, D.L. Roden, and et al. A single-cell and spatially resolved atlas of human
341 breast cancers. *Nature Genetics*, 53:1334–1347, 2021. doi: 10.1038/s41588-021-00911-1.

342

343 Z. Xu, W. Wang, T. Yang, J. Chen, Y. Huang, J. Gould, W. Du, F. Yang, L. Li, T. Lai, et al.
344 Stomicsdb: a database of spatial transcriptomic data. *bioRxiv*, pp. 2022–03, 2022. doi: 10.
345 1101/2022.03.10.483747. URL <https://doi.org/10.1101/2022.03.10.483747>.

346

347 Z. Yuan, W. Pan, X. Zhao, F. Zhao, Z. Xu, X. Li, Y. Zhao, M. Q. Zhang, and J. Yao. Sodb
348 facilitates comprehensive exploration of spatial omics data. *Nature Methods*, 20(3):387–
349 399, mar 2023. doi: 10.1038/s41592-022-01756-4. URL <https://doi.org/10.1038/s41592-022-01756-4>.

350

351 Emma Zhao, Matthew R. Stone, Xin Ren, and et al. Spatial transcriptomics at subspot
352 resolution with bayesspace. *Nature Biotechnology*, 39:1375–1384, 2021. doi: 10.1038/
353 s41587-021-00935-2. URL <https://doi.org/10.1038/s41587-021-00935-2>.

354

355 Y. Zheng, Y. Chen, X. Ding, K. H. Wong, and E. Cheung. Aquila: a spatial omics database and
356 analysis platform. *Nucleic Acids Research*, 51(D1):D827–D834, jan 2023. doi: 10.1093/nar/gkac972. URL <https://doi.org/10.1093/nar/gkac874>.

357

358 W. Zhou, M. Su, T. Jiang, Q. Yang, Q. Sun, K. Xu, J. Shi, C. Yang, N. Ding, Y. Li, et al. Sorc: an
359 integrated spatial omics resource in cancer. *Nucleic Acids Research*, 52(D1):D1429–D1437, jan
360 2024. doi: 10.1093/nar/gkad892. URL <https://doi.org/10.1093/nar/gkad820>.

361

362 Jingshu Zhu, Shiquan Sun, and Xiang Zhou. Spark-x: non-parametric modeling enables scalable and
363 robust detection of spatial expression patterns for large spatial transcriptomic studies. *Genome
364 Biology*, 22:184, 2021. doi: 10.1186/s13059-021-02404-0. URL <https://doi.org/10.1186/s13059-021-02404-0>.

365

366

367

368

369

370

371

372

373

374

375

376

377